

INVESTIGATION OF THE SURFACE CHARACTERISTICS OF AISI D3 DIE STEEL BY POWDER MIXED EDM PROCESS

BIDYUT KUMAR PANDA & SANJEEV KUMAR

Department of Mechanical Engineering, Punjab Engineering College, Chandigarh, India

ABSTRACT

Electrical Discharge Machining (EDM) is a non-conventional machining process used for machining materials that are otherwise difficult to machine by conventional processes. Powder-Mixed EDM is a variant of EDM, in which an additive powder is added to the hydrocarbon dielectric. These suspended powders affect the energy distribution and sparking efficiency, and consequently the surface finish and micro-hardness. The machining operation generates a large amount of heat. Melting and fusion of these suspended powders with carbon from the hydrocarbon dielectric occur due to the heat generated. Under appropriate machining conditions, these materials may be deposited on the machined surface resulting in surface alloying and further increase in micro-hardness. In the present work, improvement in the surface characteristics after machining of AISI high-carbon high-chromium (D3) die steel with manganese powder-mixed dielectric has been investigated. Results of the study show a significant improvement in micro-hardness and deterioration of surface finish. Scanning electron microscopy and X-ray diffraction of the machined surface indicates transfer of manganese and carbon in the form of manganese carbide. Quantitative analysis of the chemical composition of the machined surface was carried out on an optical emission spectrometer to verify the result.

KEYWORDS: EDM, Manganese Powder, AISI D3 Die Steel, Powder-Mixed Dielectric, Surface Alloying & Micro-Hardness

Received: Aug 08, 2018; **Accepted:** Aug 28, 2018; **Published:** Oct 06, 2018; **Paper Id.:** IJMPERDDEC20183

1. INTRODUCTION

EDM process is based on removing material from a part by means of a series of repeated electrical discharges between tool called the electrode, which is of a predetermined shape, and the work piece immersed in a dielectric fluid (Luis, 2005). The dielectric is generally kerosene or any other hydrocarbon oil. Short duration electric discharges of cycle time usually a few micro seconds are generated in the liquid dielectric gap that separates the tool and work piece (Fuller, 2000) (Jain, 2004). The material is removed from the tool and work piece with the erosive effect of the electrical discharges. However, by controlling the process parameters substantially more material can be removed from the work piece than the tool electrode (Shankar & Krishnan, 1979).

The electric discharges are usually of rectangular form, of magnitude 100V and frequency of the order of 200-5000Hz (Mishra, 2005). The electrode is moved towards the workpiece until the gap is small enough, so that the impressed voltage is able to ionize the dielectric (Bojorquez et al., 2002). The high frequencies of supplied voltage pulses, together with the forward movement of the tool-electrode towards the workpiece by means of a servo-mechanism, enables the sparking action to be eventually achieved over the entire area of the electrodes in contact (Ho & Newman, 2003). Unlike in conventional machining processes where the metal is removed by

mechanical action, in EDM the removal of metal is achieved by sparks. Therefore, the applicability of the process is not limited by the hardness of the metal but by its electrical conductivity. These distinctive features of EDM have ushered in the process of machining of the material in a hardened state, particularly in the manufacture of die and moulds (Altan, et al., 1993), thereby eliminating the distortions resulting from heat treatment necessary after conventional machining.

Although EDM as a machining process was developed principally for removing material from hard to machine alloys to produce desired products, nevertheless a number of phenomena observed during the process that makes it a promising technology for application in the field of surface modification (Ho & Newman, 2003). The process uses thermal energy obtained from the electric sparks produced in the gap between the tool and the workpiece in the presence of a dielectric fluid. Each spark generates a temperature of the order of $8,000^{\circ}\text{C}$ to $12,000^{\circ}\text{C}$ and creates a plasma channel, causing fusion or partial vaporization of the workpiece, tool electrode and the dielectric fluid at the point of discharge (Kuneida et al., 2005). When the plasma channel collapses at the end of pulse-on time, flowing dielectric cools the surface and carries away most of the vaporized material (Zolotikh, 1995). However, some constituents of the plasma channel are deposited back on the tool as well as the workpiece. Many researchers have reported the presence of constituents of tool electrode in the machined workpiece and vice-versa (Aspinwall, 2003). Pyrolysis of the hydrocarbon dielectric contributes carbon to the plasma channel and aids the process of material deposition (Lahiri et al., 1981). During the process, the disintegration of the electrode occurs.

For desired surface modification, the disintegrating electrode material may be deposited on the machined surface by suitably varying the process parameters towards the end of the machining cycle (Kumar et al., 2009). There is a possibility of achieving the desired surface alloying by adding suitable alloying elements, either to specially fabricated electrodes or suspending them in fine powder form in the dielectric. The alloying elements may get deposited on the machined surface either in the free form or as carbides by combining with carbon from the breakdown of the dielectric (Tzeng & Lee, 2001). Powders are suspended in the dielectric influence, the sparking pattern and machining efficiency (Jeswani, 1981). Conductive powders enlarge the gap distance and improve the surface finish by reducing the spark energy and dispersing the discharges more randomly throughout the surface (Rehbein, Schulze, Mecke, Wollenberg, & Storr, 2004). Consequently, a machined surface with thin recast layer, reduced micro-cracks, and significantly improved corrosion resistance is produced.

2. EXPERIMENTATION

This research work is undertaken to investigate the improvement in surface characteristics of AISI D3 die steel by powder mixed EDM process with manganese powder as the additive. The workpieces were EDMed with manganese powder suspended in EDM oil dielectric and material transfer from the suspended powder and carbon from the breakdown of the dielectric have been studied. The chemical composition of the workpiece material was determined by spectroscopic analysis and is given in Table 1.

Hardening of sections of reasonable size may be possible by quenching (ASM Speciality Handbook: Tool Materials, 1995), as formation of martensite of high hardness owing to 2.23% carbon in the work material together with the alloying elements can provide sufficient hardenability. Die steels exhibit poor thermal conductivity. Hence, in order to bring about uniformity in temperature to the core, the work pieces were pre-heated. The pre-heating procedure consisted of heating the work pieces to a temperature of 815°C and holding at this temperature for about 30 minutes. Subsequently, the work pieces were heated very slowly to a temperature in the range of $1000\text{--}1040^{\circ}\text{C}$ with a holding time of about 30

minutes and then quenched in still air. Immediately after quenching, the work pieces were tempered to remove the stresses of hardening and facilitate the transformation of austenite to martensite. The tempering temperature was in the range of 150-180°C. It is generally recommended to subject die steels to two cycles of tempering to remove internal stresses and to bring about uniformity in the properties. The micro-hardness of the work material was measured at five different places and the average value was found to be 710 HV (Vickers hardness number). Since the machining was to be carried out with manganese powder added to the dielectric, a small conducting tank of mild steel sheet was fabricated and placed in the main machining tank to isolate it from the filtering system. In order to keep the powder suspended uniformly in the dielectric, this tank was provided with a stirrer.

Table 1: Chemical Composition of AISI D3 Die Steel

Element	Composition (wt. %)
Carbon	2.23
Silicon	0.62
Manganese	0.65
Chromium	11.19
Molybdenum	0.26
Vanadium	0.64
Copper	0.36
Nickel	0.43
Cobalt	-
Iron	Balance

Reverse polarity (negative tool electrode) and EDM oil dielectric with side flushing was used for all experiments. Each machining operation was carried out for a period of 10 minutes. For the purpose of comparing the improvements in surface characteristics achieved with powder-mixed dielectric vis-à-vis conventional EDM, the work material was also machined with the same parameters but without any powder suspended in the dielectric medium. The average value of micro-hardness under this process was found to be 742HV.

3. EXPERIMENTAL DESIGN

Based on extensive literature survey and pilot experimentation, five input parameters (control factors), namely; electrode, peak current, pulse on-time, pulse off-time and concentration of the powder were selected for this experimental work. Non-linear behaviour of a process parameter can be studied only if more than two levels are used (Montgomery, 2005). Therefore, three levels of each parameter (factor) were taken except for electrode, which is of two levels.

The Degree Of Freedom (DOF) of a factor is defined as one less than the number of levels of the factor. Hence, the DOF of a three-level factor is 2 (Number of levels (3)-1) and two level factor is 1 (Number of levels (2)-1). In this experiment, there are four control factors of three levels and one control factor of two levels. Accordingly, the degree of freedom for the experiment is 9. Out of the standard Orthogonal Arrays (OA) available in Taguchi design of experiments, the most appropriate array, in this case, is $L_{18} (2^1 * 3^7)$ OA with 17 [= 18-1] DOF. The L_{18} orthogonal array allows one control factor with 2 levels and up to 7 control factors with three levels. Further, the orthogonality of an array is not lost, if one or more columns are not used (Phadke, 1989). Hence, L_{18} OA has been selected for running the experiment and a control log was constructed. Taguchi recommends that study of interaction should be avoided, if possible, by proper assignment of the factors. The 1st column of the L_{18} orthogonal array allows a control factor with 2 levels only. Hence, the control factor electrode, which has two levels, namely; Copper electrode and Graphite electrode has been assigned to

column 1. 2nd column of the OA was not used, as there is a possibility of interaction between column 1 and 2. The other factors, namely; peak current, pulse on-time, pulse off-time and concentration of the powder have been assigned to 3rd, 4th, 5th, and 6th columns respectively. 7th & 8th column of the OA are not used. Further, each set of eighteen experiments was repeated three times at random according to the control log for each of the work materials. The control factors (input process parameters) and their levels used for the experimentation have been listed in Table 2.

The working surfaces of the dies and press tools take the brunt of the vagaries of various operations. Hence, the micro-hardness of the working surface directly influences the quality and life of the tools; therefore, it was selected as the response parameter of the experimental work. The machined samples were subjected to micro-hardness test at a load of 9.857 N for duration of 20 seconds. The measurement was carried out at three places and the average of the three readings was taken. Further, Analysis of Variance (ANOVA) of the data was done to determine the significance and percentage contribution of each of the five factors towards improving micro-hardness. Similarly, the surface roughness of tool's influence on the lubrication condition between the tool and the formed material's surface was determined. At the same time, different surface roughness would give different friction conditions. This phenomenon plays an important role in producing a product with a glossy surface finish. Therefore, surface roughness was selected as the other response parameter and measurement of R_a value was carried out on all the samples. The samples exhibiting maximum improvement in micro-hardness were further subjected to X-Ray Diffraction (XRD) analysis to identify the presence of additional elements and the various phases; Scanning Electron Microscopy (SEM) to analyze the microstructure; and Energy Dispersive X-ray Analysis for composition testing for quantitative analysis of the changes in the constituents of the machined surface.

Table 2: Input Process Parameters and their Levels

Parameters	Units	Levels		
		L1	L2	L3
Electrode	-	Copper	Graphite	-
Peak Current	Amperes	4	6	8
Pulse on-time	μSec	21	50	100
Pulse off-time	μSec	20	40	75
Concentration	Percentage	5	10	15

4. RESULTS AND DISCUSSIONS

Micro-hardness is a higher-the-better type of response parameter. Therefore, the aim of the experiment was to maximize the value of micro-hardness. Accordingly, the signal-to-noise ratio (S/N ratio, denoted by 'η') was calculated for higher the better type (HB) as:

$$(S/N)_{HB} = -10 \log \left[\frac{1}{R} \sum_{j=1}^R \left(\frac{1}{y_j^2} \right) \right]$$

Where y_j = observed value of the response characteristic

R = Number of repetitions

A total of 54 samples were obtained after repeating each run of the control log three times. The observed values of micro-hardness and the calculated values of their S/N ratios are given in Table 3. This table also lists the average surface

roughness values (R_a) for each set of machining conditions. Further, the mean values of micro-hardness and the corresponding S/N ratios at each level of the five control factors were calculated to find out the factor effects. These factor effects have been shown in Figure 1 (a, b, c, d & e).

It is observed from Figure 1 (a) that micro-hardness shows a significant improvement with graphite electrode as compared to copper which may be due to presence of manganese carbide in the surface. Figure 1 (b) shows that micro-hardness increases with increase in peak current up to 6A and then it declines. One possible reason for this occurrence may be the decrease in surface alloying at higher values of peak current. Further, from Figure 1 (c) and Figure 1 (d) it is observed that while there is a slight improvement in micro-hardness when pulse on-time is changed from level 1 to level 2, there is substantial drop in micro-hardness for corresponding change in pulse off-time which is contrary to the established norms. This may be due to reduced energy per second with increase in pulse off-time. However, micro-hardness increases with increase in concentration (Figure 1(e)) and the maximum value is obtained at level 3 of this factor which may attributed more powder in the dielectric resulting in more surface alloying.

There are two different approaches available for complete analysis of the experimental data. While in the first method ANOVA analysis of the raw data is carried out by processing the result of a single run or the average of repetitive runs through the main effect, the second method, which Taguchi strongly recommends, use the Signal-to-Noise (S/N) ratios for the same steps in analysis (Phadke, 1989). The analysis of the data in this experimental work has been carried out by adopting the Signal-to-Noise approach. Accordingly, the results of ANOVA of the S/N data are presented in Table 4.

ANOVA of S/N data shows that all the five control factors have a significant contribution towards the response characteristics of micro-hardness. Concentration emerges as the most significant factor with a contribution of 34.72% and best micro-hardness has been obtained at level 3 of this parameter. It appears that sufficient suspended powder in the dielectric aids in better alloying of the machined surface. The contribution of peak current has been found to be the least. Highest values of micro-hardness, as can be seen from the factor effect figures (Figure. 1 (a, b, c, d & e)), has been obtained at second level of electrode (A_2) and peak current (B_2), third level of pulse on-time (C_3), first level of pulse off-time (D_1) and third level of concentration (E_3). Hence, the condition of input control factors for achieving optimum micro-hardness is A_2 , B_2 , C_3 , D_1 and E_3 . The theoretical value of η under the optimum conditions, denoted by η_{opt} , is given by

$$\eta_{opt} = m + (m_{A2} - m) + (m_{B2} - m) + (m_{C3} - m) + (m_{D1} - m) + (m_{E3} - m)$$

Where m is the overall mean of S/N data, m_{A2} is the mean of S/N data for factor A at level 2, m_{B2} is the mean of S/N data for factor B at level 2, m_{C3} is the mean of S/N data for factor C at level 3 and so on. This gives,

$$\eta_{opt} = 68.9911$$

Table 3: Observed Values of Micro-Hardness and Their S/N Ratios

Trial No.	Factor Values					Micro-Hardness Alues			S/N Ratio (η)	Average Surface Roughness, Ra (μm)
	Electrode	Peak Current (Ampere)	Pulse On-Time (μSec)	Pulse Off-Time (μSec)	Concentration (%)	R1	R2	R3		
						(HV)				
1	Copper	4A	21μs	20μs	5%	636	608	659	56.031	3.58
2	Copper	6A	50μs	40μs	10%	938	915	925	59.329	9.39
3	Copper	8A	100μs	75μs	15%	1482	1451	1469	63.331	11.76
4	Copper	4A	21μs	40μs	10%	643	660	618	56.117	5.53
5	Copper	6A	50us	75us	15%	1180	1153	1199	61.413	7.30

Table 4: Contd.,										
6	Copper	8A	100 μ s	20 μ s	5%	1140	1122	1156	61.132	9.71
7	Copper	4A	50 μ s	20 μ s	15%	1159	1172	1189	61.386	5.34
8	Copper	6A	100 μ s	40 μ s	5%	890	851	877	58.808	10.27
9	Copper	8A	21 μ s	75 μ s	10%	789	776	810	57.964	7.41
10	Graphite	4A	100 μ s	75 μ s	10%	1347	1303	1330	62.451	4.67
11	Graphite	6A	21 μ s	20 μ s	15%	1993	1970	1960	65.908	4.87
12	Graphite	8A	50 μ s	40 μ s	5%	949	913	931	59.377	7.64
13	Graphite	4A	50 μ s	75 μ s	5%	768	792	745	57.704	3.16
14	Graphite	6A	100 μ s	20 μ s	10%	2211	2244	2230	66.958	7.05
15	Graphite	8A	21 μ s	40 μ s	15%	1438	1410	1470	63.159	8.36
16	Graphite	4A	100 μ s	40 μ s	15%	1565	1603	1620	64.057	6.89
17	Graphite	6A	21 μ s	75 μ s	5%	940	922	902	59.280	3.79
18	Graphite	8A	50 μ s	20 μ s	10%	1640	1672	1649	64.367	6.92
Overall Mean						1203.28			61.043	6.87

R1, R2 and R3 represent the three repetitions

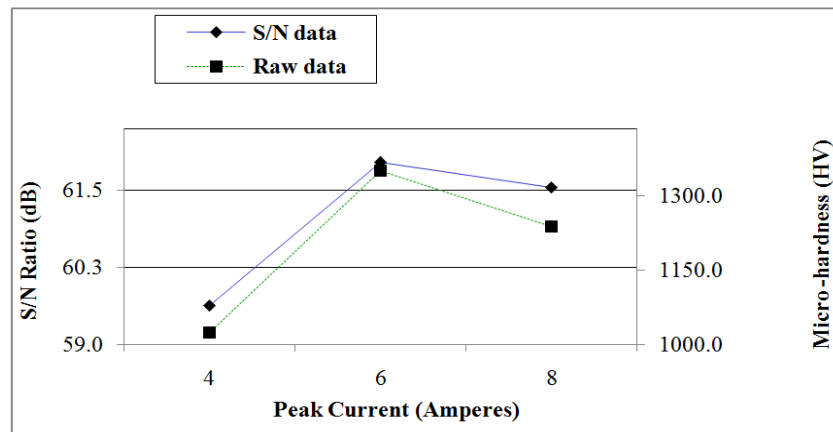


Figure 1 (a): Effect of Electrode on Micro-hardness and Its S/N Ratio

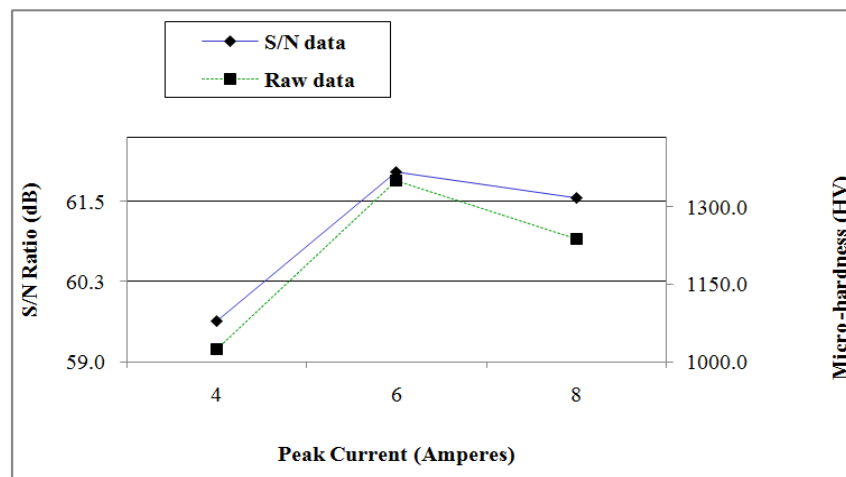


Figure 1 (b): Effect of Peak Current on Micro-hardness and Its S/N Ratio

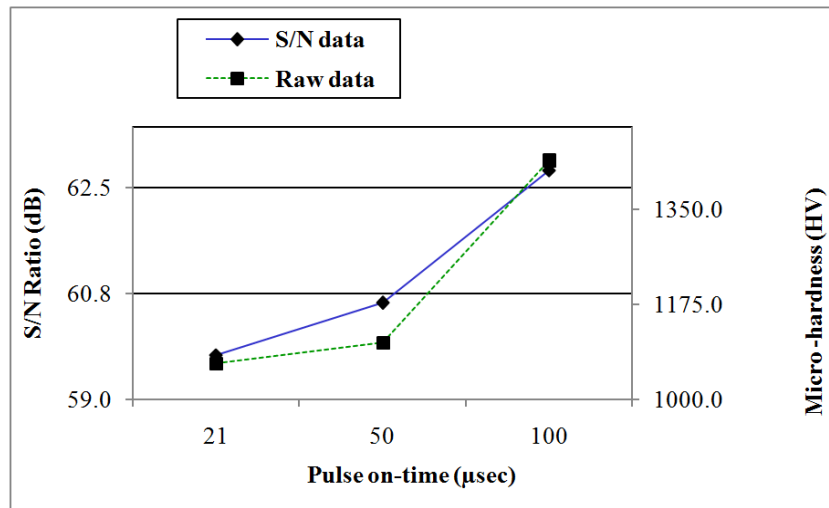


Figure 1 (c): Effect of Pulse On-Time on Micro-hardness and Its S/N Ratio

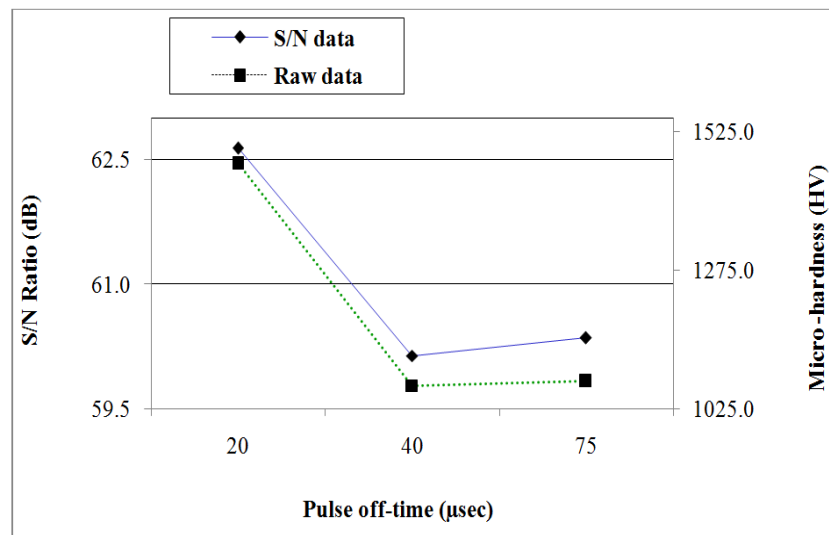


Figure 1 (d): Effect of Pulse Off-Time on Micro-hardness and Its S/N Ratio

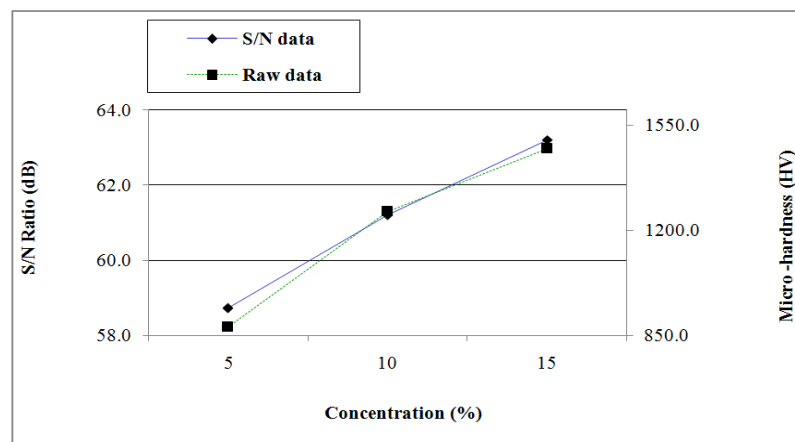


Figure 1 (e): Effect of Concentration on Micro-hardness and its S/N Ratio

Table 5: ANOVA Table of S/N Data

Factor/Parameter	Sum of Squares	DOF	Variance	F-Ratio	P %	Remarks
Electrode	42.7808	1	42.7808	2335.29	24.51	Significant
Peak Current	18.5740	2	9.2870	506.95	10.64	Significant
Pulse on-time	29.6305	2	14.8153	808.73	16.97	Significant
Pulse off-time	22.8182	2	11.4091	622.79	13.07	Significant
Concentration	60.6190	2	30.3095	1654.52	34.72	Significant
Error (Pooled)	0.1466	8	0.0183	-	0.08	-
Total	174.5692	17	-	-	100.00	-

DOF – Degrees of Freedom, P% - Percentage Contribution

Tabulated F-ratio: $F_{(0.05, 1, 8)} = 5.32$, $F_{(0.05, 2, 8)} = 4.46$ and the corresponding value of micro-hardness under these optimum conditions, y_{opt} , is calculated as

$$y_{opt}^2 = 1 / 10^{-\eta_{opt} / 10}$$

$$\text{or, } y_{opt} = 2815.51$$

This combination of input control factors for optimum condition obtained from the analysis did not exist in the orthogonal array. Therefore, a set of three experiments with these suggested optimum values were conducted. The average micro-hardness obtained from these confirmation experiments was found to be 2801.68 HV, which is very close to the theoretical value predicted by Taguchi analysis.

5. SURFACE ANALYSIS

XRD pattern of the machined surface with the maximum value of surface roughness is represented in figure 2. The XRD pattern indicates the presence of manganese carbide (Mn_7C_3) on the machined surface. The improvement in micro-hardness is due to the formation of Mn_7C_3 during machining, which has resulted from manganese combining with carbon from the electrode and dielectric during machining.

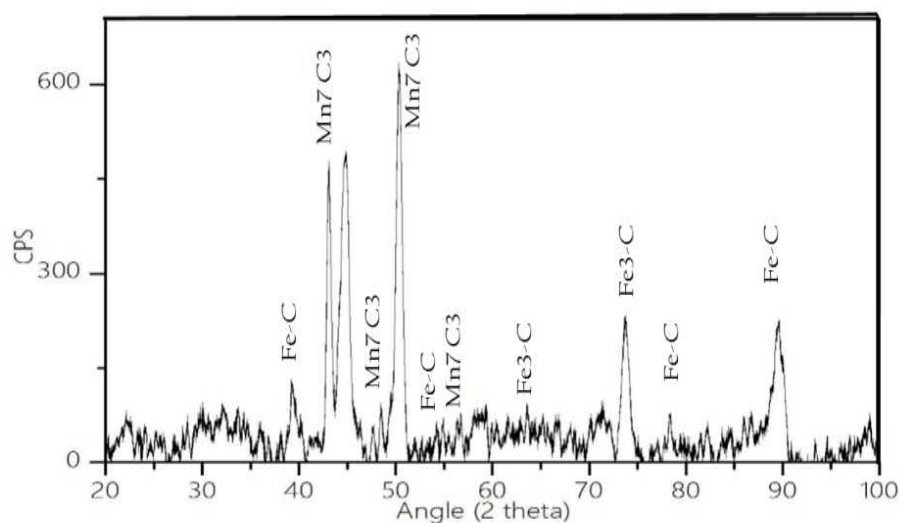


Figure 2: XRD Pattern After Machining with Manganese Powder-Mixed Dielectric

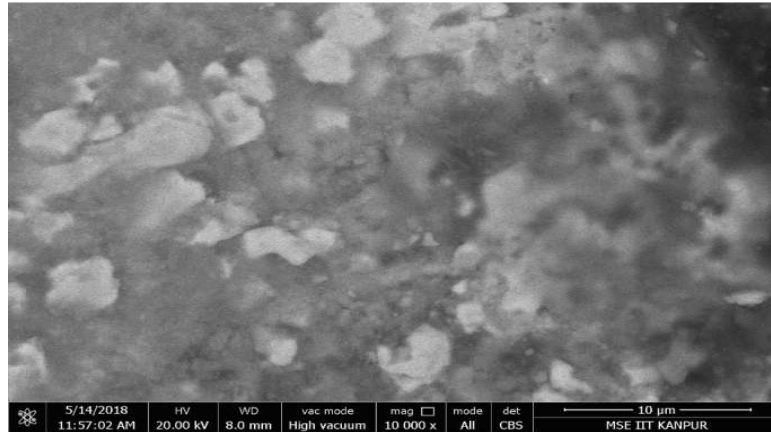


Figure 3: SEM Micrograph of the Machined Surface after Machining with Manganese Powder

The SEM micrograph of the machined surface with highest observed micro-hardness is shown in figure 3. Uniform distribution of hard particles can be seen in the micrograph. Apart from enhancing the life of the tools and dies, this may also aid in retaining lubricating oil, which is one of the desirable properties tool, and die material.

Table 5 shows the quantitative composition of elements on these surfaces before and after machining with manganese powder obtained from spectrometric analysis. An increase of about 10 to 12% in micro-hardness was observed when the work material was machined without any powder. This may be attributed to heating and quenching of the machined surface during the machining operation. This effect is more prominent with an increase in electrical energy (which is a function of peak current and pulse on-time) used for machining. Adopting machining conditions that favour material transfer result in the enhanced influence of carbon generated in the dielectric on surface hardness. The combination of control factors for optimum surface hardness for dielectric without any additive has been found to be second level of electrode (A_2), third level of peak current (B_3), third level of pulse on-time (C_3), first level of pulse off-time (D_1) and third level of concentration (E_3). The difference in the combination of control factors for optimum surface hardness without any additive and with powder mixed dielectric is only in the value of peak current; 8A for dielectric without any additive and 6A for dielectric with suspended powder. The requirement of less peak current with powder mixed dielectric may be attributed to the fact that manganese powder is already available suspended in the dielectric, whereas in case of dielectric without any additive, higher peak current means greater heating and quenching effect on the machined surface. It is observed that there is an increase in surface roughness of the machined surface produced when machined with manganese powder.

Table 6: Chemical Composition of the Material after Machining with Manganese Powder

Element	Composition (wt %)		
	Before Machining	After Machining	Significant Changes
Carbon	2.23	2.62	+0.39
Silicon	0.62	0.59	-
Manganese	0.65	1.28	+0.63
Chromium	11.19	10.91	-0.28
Molybdenum	0.26	0.31	-
Vanadium	0.64	0.61	-
Copper	0.36	0.33	-
Nickel	0.43	0.47	-

Cobalt	-	-	-
Iron	Balance	Balance	

While average surface roughness values (R_a) achieved without powder was $2.62 \mu\text{m}$ it varied from $3.16 \mu\text{m}$ to $11.76 \mu\text{m}$ with manganese powder. However, it is pertinent to mention here that some deterioration in surface finish is desirable in case of dies, as it enhances oil retention ability on the surface. Better lubrication promotes smooth functioning of the dies and prevents sticking situations between the work piece and die.

6. CONCLUSIONS

It may be concluded that surface characteristics of the machined surface can be improved by transferring significant amount of material from the powder suspended in dielectric under suitable machining parameters. In this case, it was possible to increase the percentage of manganese in the machined surface by 0.63% and carbon by 0.39%. This may be attributed to combining of carbon from the breakdown of dielectric with manganese powder suspended in the dielectric facilitated by the high temperature of the plasma channel. This is corroborated by the presence of manganese carbide (Mn_7C_3) and cementite shown in the XRD analysis.

The combination of input process parameters for optimum surface alloying from the suspended powders are found to be graphite electrode, moderate peak current (6A), longer pulse on-time (100 μsec), shorter pulse off-time (20 μsec) and high concentration of additive powder (15%). It appears that longer pulse on-time and moderate peak current together with short pulse off-time provides a large amount of energy per second which is required for the fusion of high concentration of suspended powder. Further, graphite electrode aids in providing carbon required for the formation of manganese carbide. All the five input control factors emerged as significant towards the response characteristic of micro-hardness with powder concentration emerging as the most significant factor with around 35% contribution. Another important finding of the study is that, the contribution of pulse-off time is more than peak current for the phenomenon of material transfer.

REFERENCES

1. Altan, T., Lilly, B., Kruth, J.-P., König, W., Tönshoff, H., Van Luttervelt, C., et al. (1993). *Advanced techniques for die and mold manufacturing*. CIRP Annals-Manufacturing Technology, 42 (2), 707-716.
2. ASM Speciality Handbook: Tool Materials. (1995). ASM International, USA, ISBN: 0-87170-545-1.
3. Aspinwall, D. A. (2003). *Electrical discharge surface alloying of Ti and Fe workpiece materials using refractory powder compact electrodes and Cu wire*. CIRP Annals-Manufacturing Technology, 52 (1), 151-156.
4. Astarita, G., Savage, D., & Bisio, A. (1983). *Gas Treating with Chemical Solvents*. New York: Wiley.
5. Bojorquez, B., Marloth, R., & Es-Said, O. (2002). *Formation of a crater in the workpiece on an electrical discharge machine*. Engineering Failure Analysis, 9 (1), 93-97.
6. Byer, R., & Garbuny, M. (1973). *Pollutant Detection by Absorption Using Mie Scattering and Topographic Targets as Retroreflectors*. Applied Optics, 1-10, Vol 12 No 7.
7. Chin, M., Diehl, T., Dubovic, O., Eck, T., Holben, B., & Sinyuk, A. (2009). *Light Absorption by Pollution, Dust, and Biomass Burning Aerosol: A Global Model Study and Evaluation with Aeronet Measurement*. Annales Geophysicae, 3439-3464.
8. Das, G. (2017). *Going, Going, Gone: Automation can lead to unprecedented job cuts in India*. Business Today .
9. Davidson, P. (2018). *Automation could kill 73 million U. S. jobs by 2030*. USA Today .

10. Fuji, S., Cha, H., Kagi, N., Miyamura, H., & Kim, Y. (2004). *Effects on Air Pollutant Removal by Plant Absorption and Adsorption. Building and Environment*, 105-112, Vol 40.
11. Fuller, J. E. (2000). *Electrical Discharge Machining. In ASM Machining Handbook* (pp. 16:557-564).
12. Gianto, Sarwoko, M., & Kurniawan, E. (2015). *Design Implementation Settling Dust in the High Voltage Electrostatic. e-Proceeding of Engineering*, 2091-2098, Vol. 2 No. 2.
13. Ho, K., & Newman, S. (2003). *State of the art electrical discharge machining (EDM). International Journal of Machine Tools and Manufacture*, 43 (13), 1287-1300.
14. Jain, V. K. (2004). *Advanced Machining Processes. Allied Publishers, New Delhi, ISBN: 81-7764-294-4.*
15. Jeswani, M. L. (1981). *Effect of the addition of graphite powder to kerosene used as the dielectric fluid in electrical discharge machining. Wear* , 70, 133-139.
16. Kumar, S., Singh, R., Singh, T. P., & Sethi, B. L. (2009). *Surface modification by electrical discharge machining: a review. Journal of Materials Processing Technology*, 209 (8), 3675-3687.
17. Kunieda, M., Lauwers, B., Rajurkar, K., & Schumacher, B. (2005). *Advancing EDM through fundamental insight into the process. CIRP Annals-Manufacturing Technology*, 54 (2), 64-87.
18. Lahiri, B., Mukherjee, S., & Mullick, B. (1981). *Loss of energy in pyrolysis of dielectric in EDM process. J. Inst. Eng.(India)*, 62, 66-69.
19. Luis, C. J. (2005). *Material removal rate and electrode wear study on the EDM of silicon carbide. Journal of Material Processing Technology* (164), 889-896.
20. Mahendra, S., Qomaruddin, M., & Mulyahati, M. (2017). *Studi Penyaring Emisi pada Kanlpot Sepeda Motor dengan Briket Arang Batok Kelapp. Traksi* , 1-13, Vol 17 No 2.
21. Mishra, P. K. (2005). *Non Conventional Machining. Narosa Publishing House. ISBN: 81-7319-192-1.*
22. Montgomery, D. (2005). *Design & Analysis of Experiments* (5th ed.). John Wiley & Sons, ISBN 9971-51-329-3.
23. Phadke, M. (1989). *Quality engineering using robust design. AT & T Bell Laboratories, P T R Prentice Hall Inc, New Jersey, USA, ISBN 9971-51-329-3.*
24. Pope, D., Mishra, V., Thompson, L., Siddiqui, A., Rehfuess, E., & Weber, M. (2010). *Risk of Low Birth Weight and Stillbirth Associated with Indoor Air Pollution from Solid Fuel Use in Developing Countries. USA: Epidemiologic Review*, 70-81, Vol 32.
25. Popescu, I., Stihi, C., Cimpoca, G., Dima, G., Vlaicu, G., & Gheboianu, A. (2009). *Environmental Samples Analysis by Atomic Absorption Spectrometry (AAS) and Inductively Coupled Plasma-Optical Emission Spectroscopy (ICP-AES). Romamnia Journal Physic*, 1-6, Vol 54.
26. Price, R. (2017). *Stephen Hawking: This will be the impact of automation and AI on jobs.*
27. Rehbein, W., Schulze, H. P., Mecke, K., Wollenberg, G., & Storr, M. (2004). *Influence of selected groups of additives on breakdown in EDM sinking. Journal of Materials Processing Technology*, 149 (1-3), 58-64.
28. Ruhiat, Y. (2009). *Model Prediksi Distribusi Laju Penyebaran Pencemar SO2 dan Debu dari Kawasan Industri Cilegon. Bogor: IPB.*
29. Shankar, N., & Krishnan, A. (1979). *Polarity effect in spark erosion machining. Indian J. Technol.*, 17 (9), 363-364.

30. Soerjono. (2015). *Laporan Kinerja Kementerian Perindustrian*. Jakarta: Kementerian Perindustrian Indonesia.
31. Syakur, A., Warsito, A., & Nurlailati. (2009). Aplikasi Tegangan Tinggi DC sebagai Pengendap Debu secara Elektrostatis. *Teknologi Elektro*, 38-45, Vol. 8 No. 1.
32. Tyson, L. (2017). *The future is automated, but what does that really mean for jobs?*
33. Tzeng, Y.-F., & Lee, C.-Y. (2001). Effects of powder characteristics on electrodischarge machining efficiency. *The International Journal of advanced manufacturing technology*, 17 (8), 586-592.
34. Verlina, W., Wahab, A., & Maming. (2018, July Friday). Potensi Arang Aktif Tempurung Kelapa sebagai Adsorben Emisi Gas CO, NO dan NOx pada Kendaraan Bermotor. Retrieved from file:///C:/Users/Hp/Downloads/Documents/wa%20odeveby%20verlina.pdf: file:///C:/Users
35. Wahyuningrum, A., Wardoyo, A., & Darmawan, H. (2018, July Friday). Sistem Filtrasi Berbahan Serabut Kelapa untuk Emisi Partikulat PM2.5 dari Sepeda Motor. Retrieved from <https://media.neliti.com/media/publications/161227-ID-sistem-filtrasi-berbahan-serabut-kelapa-pdf>: <https://media.neliti.com>
36. Zannetti, P. (1990). *Air Pollution Modeling: Theories, Computational Methods and Available Software*. New York: Computational Mechanics, pp. 162-167.
37. Zolotikh, B. (1995). Modern physical theory of electric erosion of metals-the basis for development of new directions in EDM. *Proceedings of the International Symposium on Electromachining-XI*, (pp. 114-116).